DOI: 10.1002/adma.200501961

Design and Creation of Superwetting/Antiwetting Surfaces

By *Xinjian Feng* and *Lei Jiang**

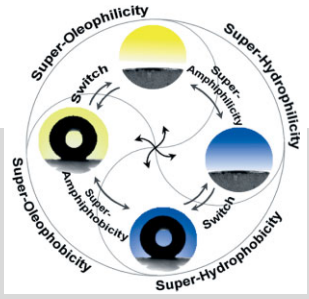

Recent achievements in the construction of surfaces with special wettabilities, such as superhydrophobicity, superhydrophilicity, superoleophobicity, superoleophilicity, superamphiphilicity, superamphiphobicity, superhydrophobicity/superoleophilicity, and reversible switching between superhydrophobicity and superhydrophilicity, are presented. Particular attention is paid to superhydrophobic surfaces created via various methods and surfaces with reversible superhydrophobicity and superhydrophilicity that are driven by various kinds of external stimuli. The control of the surface micro-/nanostructure and the chemical composition is critical for these special properties. These surfaces with controllable wettability are of great importance for both fundamental research and practical applications.

1. Introduction

The wetting behavior of solid surfaces by a liquid is a very important aspect of surface chemistry, which may have a variety of practical applications.[1–7] When a liquid droplet contacts a solid substrate, it will either remain as a droplet or spread out on the surface to form a thin liquid film, a property which is normally characterized using contact angle (CA) measurements. For a solid substrate, when the CA of water or oil on it is larger than 150°, it is called superhydrophobic or superoleophobic, respectively.[8] On the other hand, when the CA of water or oil on a surface is almost 0°, it is called superhydrophilic or superoleophilic, respectively.[9]

Inspired by superhydrophobic living organisms in Nature, such as lotus leaves[10,11] and water-strider legs,[12] artificial surfaces with superhydrophobicity and superoleophobicity are commonly fabricated via two kinds of approaches: creating micro-/nanostructures on hydrophobic substrates, or chemically modifying a micro-/nanostructured surface with materials of low surface free energy.[11] In this way, various methods for attaining surface roughness have been proposed, such as crystallization control,[13] phase separation,[14,15] electrochemical deposition,[16,17] and chemical vapor deposition.[18] Superhydrophilic and superoleophilic surfaces have also been fabricated via increasing both the surface roughness and the surface free energy. The mechanism here is commonly referred to as a 2D[9] or 3D[19] capillary effect.

Based on these fundamental wetting properties, that is, superhydrophobicity, superhydrophilicity, superoleophobicity, and superoleophilicity, other kinds of surface functions can be obtained by combining any two (illustrated in Fig. 1). For a solid substrate with micro-/nanostructures and a very high surface free energy, superhydrophilicity and superoleophilicity can coexist, and the film will show superamphiphilicity[7] (Fig. 1, right). For a rough surface with a very low surface free energy, superhydrophobicity and superoleophobicity can coexist, and the film will show superamphiphobicity[20] (Fig. 1, left). Analogously, when superhydrophobicity/superoleophobicity or superhydrophilicity/superoleophobicity coexist (Fig. 1, center), separation of water from oil (or oil from water) can be realized.[21] In addition to surfaces with these static wetting properties, in some cases the surface chemical composition or geometrical structure of a rough surface can be tuned dynamically. In such a case, a smart surface whose wettability can be modulated reversibly between superhydrophobicity and superhydrophilicity (Fig. 1, top) or superoleophobicity and superoleophilicity (Fig. 1, bottom) is obtained.

[*] Prof. L. Jiang
Institute of Chemistry, Chinese Academy of Sciences
National Center for Nanoscience and Nanotechnology
Beijing 100080 (P.R. China)
E-mail: jianglei@iccas.ac.cn
X. J. Feng
Institute of Chemistry, Chinese Academy of Sciences
Graduate School of the Chinese Academy of Science
Beijing 100080 (P.R. China)

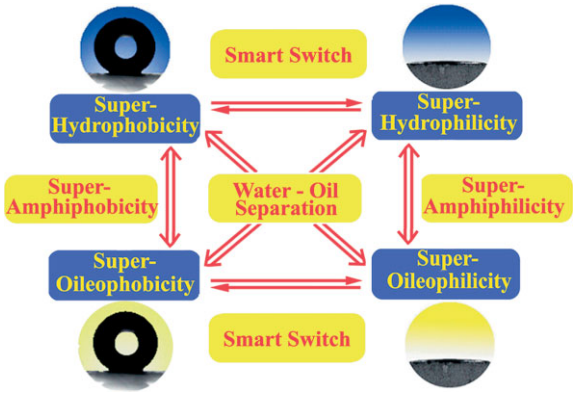

Figure 1. Illustration of the relationships between the four kinds of fundamental superwetting/antiwetting properties (in blue boxes) and the further special surface superwetting/antiwetting functions (in yellow boxes) that are obtained by combining either two of the fundamental properties. Herein, the double arrow indicates coexistence of the two properties, and the reversible arrow indicates switching of the two properties.

The wettability of solid substrates is governed by their surface free energy and surface geometrical structure. Therefore, dynamically changing one of these two factors can be used to modulate the surface wettability.[3,22,23] The surface free energy of stimuli-responsive materials depends on their environment.[24–29] Recently, through the modification of stimuli-responsive materials on substrates with appropriate surface geometric structures, remarkable surface wettabilities that can be reversibly switched between superhydrophobicity and superhydrophilicity have been realized.[30–35] On the other hand, for a surface with a given surface free energy, tuning the surface geometrical structure has also been used to control the surface wettability.[36] These wettability switchable surfaces can be used for the construction of future-generation smart devices.

The subjects to be covered in the following sections are functional surfaces with special wettability. In Sections 2 and 3, we review the fundamental theories and various methods for the preparation of superhydrophobic surfaces. In the next three sections, surfaces with superamphiphobicity, superamphiphilicity, and superhydrophobicity/superoleophilicity are presented successively. Then, we focus on superhydrophobic and superhydrophilic reversible-switch surfaces, which are the highlight of this Review. Finally, we provide our conclusions and outlook on the future of this research.

2. Fundamental Theories

For a liquid droplet on a flat film (Fig. 2a), the wettability is determined by the surface free energy of a solid substrate, which is commonly given by the Young's equation (Eq. 1)

$$\cos\theta = (\gamma_{sv}-\gamma_{sl})/\gamma_{lv} \quad (1)$$

where θ is the contact angle in the Young's mode, and γ_{lv}, γ_{sv}, and γ_{sl} are the different surface tensions (liquid/vapor, solid/vapor, and solid/liquid) involved in the system. In actuality,

Lei Jiang is currently a professor at the Institute of Chemistry, Chinese Academy of Sciences (ICCAS). He received his B.Sc. degree in physics (1987) and M.Sc. degree in chemistry (1990) from the Jilin University of China. From 1992 to 1994, he studied in Tokyo at the University of Japan as a China–Japan joint course Ph.D. student and received his Ph.D. degree from Jilin University of China with Prof. Tiejin Li as his supervisor. He then worked as a postdoctoral fellow in Prof. Akira Fujishima's group at Tokyo University. In 1996, he worked as a senior researcher at the Kanagawa Academy of Sciences and Technology under Prof. Kazuhito Hashimoto. He joined ICCAS as part of the Hundred Talents Program in 1999. Today, he is also a chief scientist of the National Center for Nanoscience and Technology of China. His scientific interests are focused on bio-inspired surfaces and interfacial materials.

Xinjian Feng is currently a Ph.D. student at ICCAS. He received his B.Sc. degree in chemistry from Jilin University, China in 1998. From 1998 to 2001, he successively worked as an assistant engineer for the Lucky Film Co. Ltd. and as an engineer at the ShenZhen Tsinghua Rainbow Co. Ltd. of China. In 2001, he joined Prof. Lei Jiang's group at ICCAS and received his M.Sc. degree in 2003. His current scientific interests are focused on synthesizing and assembling low-dimensional semiconducting nanomaterials and understanding their structure-related special surface physical and chemical properties.

ADVANCED MATERIALS

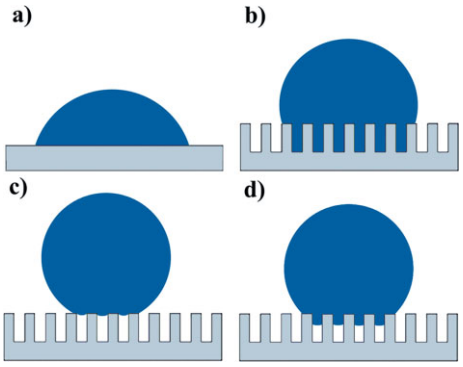

Figure 2. Effect of surface structure on the wetting behavior of solid substrates. a) A liquid drop on a flat substrate (Young's mode). b) Wetted contact between the liquid and the rough substrate (Wenzel's mode). c) Non-wetted contact between the liquid and the rough substrate (Cassie's mode). d) Intermediate state between the Wenzel and the Cassie modes.

few solid surfaces are truly flat; therefore, the surface roughness factor should also be considered during the evaluation of the surface wettability. The theories that are commonly used to correlate the surface roughness with the apparent CA of a liquid droplet on a solid substrate are the Wenzel and Cassie equations.

2.1. Wenzel's Theory

In the Wenzel case,[1] as illustrated in Figure 2b, the liquid completely fills the grooves of the rough surface where they contact, described by Equation 2

$$\gamma_{lv} \cos\theta_W = r\,(\gamma_{sv} - \gamma_{sl}) \tag{2}$$

where θ_W is the apparent CA in the Wenzel mode and r is the surface roughness factor. Combining Equation 2 with Equation 1 yields Equation 3

$$\cos\theta_W = r\cos\theta \tag{3}$$

From Equation 3, it can be found that if the CA of a liquid on a smooth surface is less than 90°, the apparent angle on a rough surface will be smaller, while for a true CA > 90°, the angle on a rough surface will be larger. These two situations can be described as: for $\theta < 90°$, $\theta_W < \theta$; for $\theta > 90°$, $\theta_W > \theta$.

2.2. Cassie's Theory

In the Cassie theory,[2] vapor pockets are assumed to be trapped underneath the liquid, which gives a composite surface (Fig. 2c). Defining the apparent CA in the Cassie mode as θ_C, θ_C can be correlated to the chemical heterogeneity of a rough surface by Equation 4

$$\cos\theta_C = f_s\cos\theta_s + f_v\cos\theta_v \tag{4}$$

where f_s and f_v are the area fractions of the solid and vapor on the surface, respectively. Since $f_s + f_v = 1$, $\theta_s = \theta$, and $\theta_v = 180°$, Equation 4 can be written as Equation 5

$$\cos\theta_C = -1 + f_s\,(\cos\theta + 1) \tag{5}$$

Typically, if a surface exhibits fractal structures, Equation 5 can be modified to produce Equation 6[37]

$$\cos\theta_C = -1 + f_s\left(\frac{L}{l}\right)^{D-2}(\cos\theta + 1) \tag{6}$$

where L and l are the upper and lower limits of fractal behavior, respectively, and D is the fractal dimension.

From Equations 5 and 6 it can be found that for a true CA > 90°, the surface roughness will increase the apparent angle. This is unlike the Wenzel case, because even when the intrinsic CA of a liquid on a smooth surface is less than 90°, the contact angle can still be enhanced as a result of the as-trapped superhydrophobic vapor pockets.

2.3. Transition Between Cassie's and Wenzel's States

According to Equations 3 and 5, for a surface with the same roughness, there should exist two distinct apparent CAs. It has also been reported that the solid/liquid contact mode will change from the Cassie to the Wenzel state when the spherical liquid droplet is pressed physically.[38–40] This indicates that in addition to coexisting, a transition between these two superhydrophobic states can also occur[41–44] (Fig. 1d). When the wetting behavior changes from the Cassie mode to the Wenzel mode, the liquid droplet will fill the grooves of the rough substrate with a decrease in the apparent CA, and Equations 5 and 3 should be obeyed before and after the transition, respectively,. Equating these two results, the threshold value θ_{T1} between the two modes can be obtained as Equation 7[45]

$$\cos\theta_{T1} = (f_s - 1)/(r - f_s) \tag{7}$$

where the subscript T1 denotes that θ_{T1} is a threshold value between the Wenzel and Cassie modes.

If the Young's CA is lower than the threshold value given by Equation 7, the as-trapped vapor pockets are metastable and the Wenzel mode will be obtained. For the apparent CA of a liquid droplet to agree with the Cassie mode, the solid substrate must be hydrophobic enough or θ_{T1} must be as small as possible, because only when $\theta > \theta_{T1}$ are the as-trapped vapor pockets stable.

2.4. Dynamic Wetting Behavior

The hydrophobicity of the surface is commonly measured by the apparent water CA, which is the static behavior of a liquid droplet. Besides this, the rolling-off or sliding-down behavior of liquid droplets is another criterion for the evaluation of the repellency of a surface. The sliding behavior of a liquid droplet is evaluated by measuring the sliding angle, α, at which a liquid droplet begins to slide down an inclined plate. Commonly, a surface with a large static CA does not have droplets slide off it easily due to the contact-angle hysteresis.[46,47] The quantitative relationship between the CA hysteresis and the sliding angle is given by Equation 8[48]

$$mg(\sin\alpha)/w = \gamma_{lv}(\cos\theta_R - \cos\theta_A) \quad (8)$$

where θ_A and θ_R are the advancing and receding contact angles, respectively, g is the force due to gravity, and m and w are the mass and width of the droplet, respectively. From Equation 8, it can be found that a lower droplet weight and smaller difference between the advancing and receding contact angles will result in a smaller α.

The surface roughness has a strong effect on the CA hysteresis.[46] When the surface hydrophobicity is governed by the Wenzel mode, the liquid droplet on it will remain unmoved even if the film is tilted to a significant angle, whereas it slides off easily even if the film is only slightly tilted when the hydrophobicity is governed by the Cassie mode. According to the Johnson and Dettre simulation,[49] the contact mode can be switched continuously from Wenzel to Cassie modes with increasing surface roughness. Therefore, increasing the surface roughness can be used to lower the sliding angle. The sliding behavior of a liquid droplet is also governed by the movement of the three-phase contact line toward its sliding direction.[50,51] A short continuous contact line is favorable for surfaces with a low sliding angle or low CA hysteresis. Therefore, in order to prepare surface with a high water CA and low sliding angle (SA), an effective design takes into account not only the surface roughness but also the surface geometrical structure.

The driving force (F) needed to start a liquid drop moving over a solid surface is commonly adopted to evaluate the CA hysteresis, given by Equation 9[52]

$$F = \gamma_{lv}(\cos\theta_R - \cos\theta_A) \quad (9)$$

External forces (wind, gravity, etc.) can be employed to overcome the hysteresis if F is small. Such a mechanism has been employed by some beetles to capture water in the desert.[53] Water microdroplets in the fog that strike the hydrophobic region of the elytra (anterior wings of beetles) can be blown off easily by the wind and collected. The static and dynamic properties described in this section are the basic wetting behaviors of liquid droplets on solid surfaces. Based on these mechanisms, in the following sections, we will introduce various methods that are employed to design surfaces with controlled wettability.

3. Superhydrophobic Surfaces

3.1. Superhydrophobic Surfaces in Nature

During the past decade, studies on many biological surfaces have revealed that a macroscopically smooth surface commonly exhibits a microscopic roughness on different length scales.[10,11,53–56] The surface micro- and nanostructures together with hydrophobic epicuticular wax crystalloids lead to superhydrophobicity. The superhydrophobicity of lotus leaves has been known for a long time. Water droplets are almost spherical on them and roll off easily, which is usually referred to as the "lotus effect". Superhydrophobicity of lotus leaves was first revealed by Barthlott and Neinhuis.[10] It was reported that this unique property is caused by the surface micrometer-sized papillae. However, detailed scanning electron microscopy (SEM) images of lotus leaves (Fig. 3) indicate that their surfaces are composed of micro- and nanometer-scale hierarchical structures, that is, fine-branched nanostructures (ca. 120 nm) on top of micropapillae (5–9 μm).[11] The cooperation of these special double-scale surface structures and hydrophobic cuticular waxes is believed to be the reason for the superhydrophobicity, i.e., a high water CA and low SA. A similar superhydrophobic property was also observed on the leaf of "lady's mantle", a herbaceous perennial plant.[57,58]

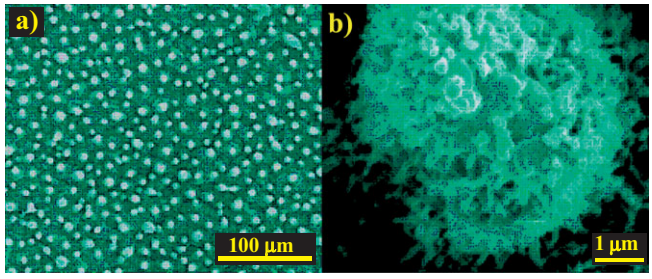

Figure 3. A superhydrophobic lotus leaf. a) Low- and b) high-magnification SEM images of the surface structures on the lotus leaf. Every epidermal cell forms a micrometer-scale papilla and has a dense layer of epicuticular waxes superimposed on it. Each of the papillae consists of branchlike nanostructures. Reprinted from [11].

In addition to the leaves of plants, many insects,[12,59,60] such as the water strider, butterfly, and the cicada, also show superhydrophobicity. Water striders (Fig. 4) are remarkable in that their nonwetting legs that enable them to stand effortlessly on water.[10] The maximal supporting force of a single leg is 152 dyn (1 dyn = 1×10^{-5} N), which is about 15 times the weight of the insect. SEM imaging revealed that the leg is composed of numerous needle-shaped setae with diameters on the microscale and that each microseta is composed of many elaborate nanoscale grooves (Fig. 4b). Such a hierarchical surface structure together with the hydrophobic, secreted wax is considered to be the origin of the superhydrophobicity of the water strider's legs.

ADVANCED MATERIALS

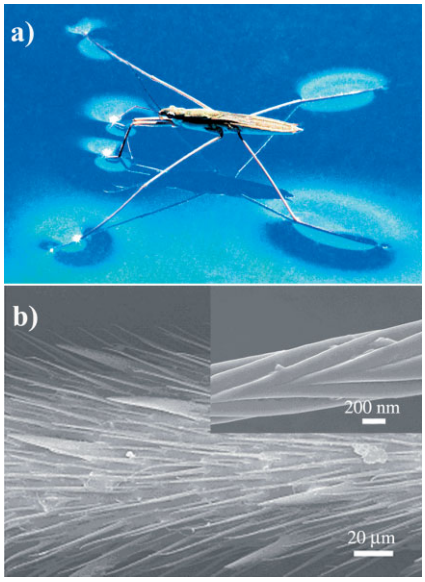

Figure 4. The superhydrophobic legs of the water strider (*Gerris remigis*). a) Photograph of a water strider standing on the water surface. b) SEM image of the leg with oriented spindly microsetae. The inset in (b) shows the nanoscale groove structure on a single seta. Reprinted with permission from [12]. Copyright 2004 Nature Publishing Group.

Butterflies[59] and cicadae[60] (Fig. 5a) can keep themselves uncontaminated by removing dust particles, dew, or water droplets easily from their wings. Such properties also originate from the special microstructures on their wings. The cicada wing is composed of aligned nanocolumns with diameters of about 70 nm and a column-to-column distance of about 90 nm (Fig. 5). These surface microstructures bestow the wing with its self-cleaning property.

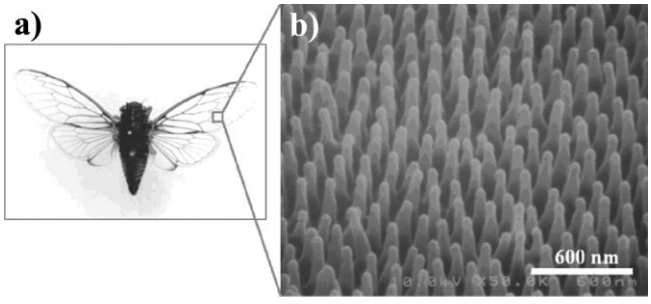

Figure 5. a) *Cicada orni* and b) field-emission SEM image of the surface nanostructure on its wing, showing regularly aligned nanoposts. Reprinted with permission from [60]. Copyright 2004 American Chemical Society.

3.2. Artificial Superhydrophobic Surfaces

Research on the surface of plant leaves and insects reveals the importance of surface micro- and nanostructures for the superhydrophobicity observed. Based on this, various approaches have been proposed for the preparation of superhydrophobic surfaces via the construction of an appropriate surface-geometry structure.

3.2.1. Template Synthesis

Template synthesis is an effective means to construct surface structures.[61–66] Among these templates, nanoporous anodic aluminum oxide (AAO) has been widely used for pressure-driven imprint processes. The diameter and height of the projecting surface nanostructure can be controlled by using AAO replications with different pore diameters and channel lengths, respectively. Based on such a template, a simple "template rolling press" method for preparing large-area, well-aligned, polycarbonate nanopillar arrays with superhydrophobicity was reported.[62] In addition, a "template-based extrusion technique" for fabricating aligned polymer nanofiber films was also developed,[63,64] in which only the extrusion under pressure of the polymer solution through the channels of the AAO template is necessary.

Another kind of commonly used templates are polystyrene (PS) and silica spheres.[65,66] Nanosphere lithography is a well-established technique for patterning periodic nanopore arrays over large areas. After depositing thin films of various materials onto the sacrificial template, the spherical colloid particles are removed, which leaves the porous shells intact. It is important to note here that the self-assembly of colloid particles on a solid substrate itself can also serve as a rough surface structure, and has already been employed to construct superhydrophobic surfaces.[67,68]

3.2.2. Phase Separation

In this method, a hardening process is adopted to produce porous materials that consist of a solid phase and a second phase that could be liquid or solid. After the second phase is removed, a porous rough surface is obtained.[14,15] To simplify this, a one-step method to prepare superhydrophobic surfaces based on phase separation has recently been reported,[69] in which a porous surface with high roughness can be obtained without removing the second phase. Recently, Han et al.[70] selected supramolecular organosilane, which is present in a phase-separated state in solution, to prepare superhydrophobic surfaces. In their method, neither a hardening process nor any other additives are required.

3.2.3. Electrochemical Deposition

Electrochemical deposition (ECD) is a facile and inexpensive method to construct rough surfaces regardless of the size and shape of the substrate. For the construction of highly rough surface structures using ECD, a two-step approach is commonly adopted. First, a small electrical potential is used to create small nanoparticles on the substrate, followed by an overpotential deposition used to produce larger and extended metal nanostructures. Based on this method, copper films of

varying levels of roughness were prepared.[71] To extend and simplify this two-step ECD method, Zhang and co-workers reported the formation of fractal metal clusters through the combination of layer-by-layer (LbL) deposition and ECD.[16,72] An indium tin oxide electrode or gold thread is modified with polyelectrolyte multilayers through the LbL method, and then, a metal, such as gold or silver, is electrodeposited onto the multilayers to form dendritic rough structures. It can be deduced that if a micrometer-sized surface structure is formed on the electrode before ECD, a micro- and nanometer hierarchically rough surface can be obtained after ECD. This idea was demonstrated by the recent work of Shirtcliffe et al.[17] These films show superhydrophobicity after the as-deposited films were modified with a hydrophobic molecular layer.

In addition to metal, by controlling the reaction conditions, inorganic semiconductor and conducting polymer films with various surface structures can also be fabricated via the electrochemical method. Recently, an array of needlelike microtubes of conductive poly(alkylpyrrole) were electrochemically synthesized (Fig. 6).[73] The arrays of the fractal surface structure endow the film with its superhydrophobicity. Similarly, Zhang et al. prepared aligned ZnO nanorod films. After modification with a monolayer of fluoroalkylsilane, the film had a water CA larger than 150°.[74]

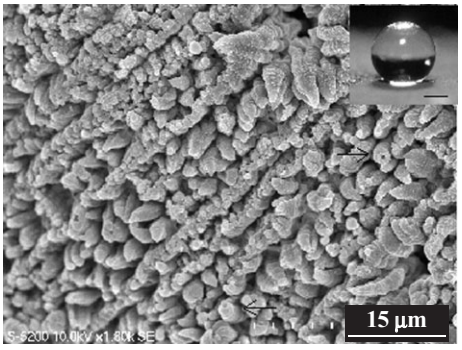

Figure 6. SEM image of an aligned poly(alkylpyrrole) microtube film prepared via the ECD method. The inset shows a water droplet on the film (scale bar: 500 μm). Reprinted from [73].

3.2.4. Electrohydrodynamics

Electrohydrodynamics (EHD) is a versatile technique that has been used to manufacture fibers with diameters ranging from micrometers to nanometers.[75–77] In a typical EHD process, a high voltage is applied to a nozzle through which the sample solution is pumped. Because of the evaporation of the solvent, the solution jet solidifies and forms a rough film on the collector. The morphology of the EHD products is strongly influenced by the concentration of the solution.[75] When a highly concentrated solution is used, the high viscosity is sufficient to sustain the elongation of the solution jet, and films that consist of ultrafine fibers are formed, while for dilute solutions, the thin jet of solution will shrink to droplets and form microparticles. For all conditions in between, porous nanofibers/microspheres composite 3D network structures can be obtained (Fig. 7). In addition to the solution viscosity, the surface-charge density also strongly influences the morphology of the nanofibers.[76,77] During the electrospinning process, a higher surface charge density on the solution-jet surface will result in smaller beads and thinner fiber diameters.

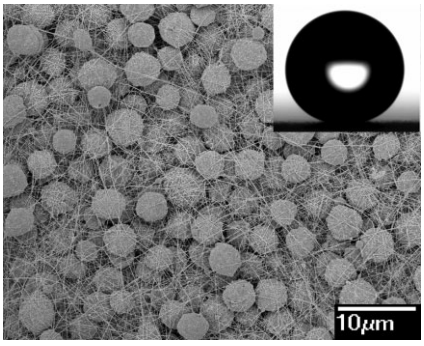

Figure 7. SEM images of superhydrophobic polystyrene films with special microsphere/nanofiber composite structures prepared via the EHD method. Reprinted from [75].

3.2.5. Crystallization Control

Controlling the crystallization of materials can result in rough surface structures, and was firstly adopted by Tsujii and co-workers to prepare superhydrophobic surfaces.[78] An alkyl ketene dimer (AKD) was first melted at high temperature and then cooled to room temperature. During the cooling process, a fractal AKD rough surface with superhydrophobicity was obtained. By controlling the solvent-evaporation temperature, the crystallization time, the nucleation rate, the surface-roughness factor, and the water CA can be controlled. Erbil et al. dissolved isotactic polypropylene using an appropriate solvent at high temperature.[79] As the temperature decreased, the polymer crystallized into a gel-like porous structure, which induced a water CA as high as 160°. Recently, superhydrophobic low-density polyethylene films have also been fabricated by controlling the surface crystallization behavior.[80]

The methods mentioned above are some of the convenient approaches for the construction of special rough surfaces with superhydrophobicity. In addition to these, many other methods have also been developed, including chemical vapor deposition (CVD),[18,81] plasma polymerization/etching of polymer films,[82,83] laser ablation and photolithography-based microfabrication,[84] self-assembly,[85–87] glancing-angle deposition,[88] and wet chemical deposition routes.[89–91]

3.3. Multifunctional Superhydrophobic Surfaces

Although surfaces with superhydrophobicity have been fabricated via various approaches, for practical industrial pro-

cesses and our daily life, many other important functions are desired besides superhydrophobicity. In addition, by increasing the surface roughness, many other important properties of the solid substrate can be lost. For example, the optical transparency and the mechanical stability decrease, greatly limiting the widespread application of superhydrophobic surfaces. Therefore, much attention has been devoted to the fabrication of multifunctional superhydrophobic films.

3.3.1. Superhydrophobic Surfaces with Optical Properties

Optical transparency is of special importance for many devices (eyeglasses, automobile windows, etc.). However, hydrophobicity and transparency are two competing properties in view of the surface roughness. Increasing the surface roughness can enhance the hydrophobicity, whereas the transparency decreases due to light-scattering losses. Therefore, controlling the surface roughness to an appropriate value is the key point to satisfy both needs.[92]

Tadanaga et al.[93] and Nakajima et al.[94] developed a sol–gel method for producing transparent boehmite films on glass substrates. The surface roughness could be precisely controlled in the range between 20 and 50 nm. However, this method requires a high-temperature process (> 400 °C), which is incompatible with many optical devices. To solve this problem, a microwave plasma-enhanced CVD process was adapted to fabricate transparent superhydrophobic films at temperatures as low as 100 °C.[95,96] Very recently, we prepared multifunctional ZnO nanorod films with visible-light transparency and superhydrophobic properties through controlling the diameter and length of nanorods using a low-temperature solution approach.[97] The diameter and the spacing between the nanorods are both less than 100 nm. Such surface nanostructures are small enough not to give rise to visible light scattering.

Another very important optical function of thin films is conferral of antireflective (AR) properties, important in fabricating eyeglasses, cover glasses for solar cells, and many other optical instruments. Although the methods for preparing AR films have been extensively studied, only a few examples have been reported for the fabrication of AR films with superhydrophobicity. Xu et al. developed a procedure to prepare superhydrophobic AR films using methyl-modified SiO_2 sols.[98,99] The water CA reached 165°, and the lowest reflectivity on one-side films reached 0.03 %. Recently, Zhang and coworkers reported the combination of AR and self-cleaning properties in a core/shell-like TiO_2/SiO_2 particle coating.[100] Park et al. showed that spin-coating of a polymer/solvent/non-solvent ternary system on glass exhibits excellent AR properties.[101] However, the wettability of these films is merely hydrophobic, with a CA of about 120°. Therefore, in order to fabricate superhydrophobic films with good AR properties, further work can be done to decrease the surface free energy while maintaining the surface roughness.

UV light is very harmful to skin as well as many kinds of organic compounds. For practical applications, UV-protective and visible-light transparent superhydrophobic films are needed. To protect something from UV light, inorganic semiconductors that absorb UV light are the first materials selected because of their wide optical bandgap. However, after long-term outdoor exposure, the films lose their superhydrophobicity gradually and irreversibly because of their strong photocatalytic property.[102] Considering this, opal or inverse-opal films made of a material without photocatalytic properties can be chosen.[103] The stop band of the films can be easily engineered to the UV region by changing the diameter of the spheres. As a result, the incident UV-light wavelength lies within the stop band and is, thus, reflected.

3.3.2. Superhydrophobic Surfaces with Highly Adhesive Forces

As discussed in Section 2.4, it is commonly acknowledged that a surface with a high water CA and small contact area should be associated with a low SA and adhesive force. However, recent research on superhydrophobic surfaces indicates that it is not an axiom.[104] The film in Figure 8a and b shows superhydrophobicity, while it can hold a spherical water droplet even when it is turned upside down. The maximum adhesive force is about 59.8 μN, as assessed by a high-sensitivity microelectromechanical balance system. A detailed SEM image (Fig. 8c) shows that the as-prepared PS films are composed of about 6.76×10^6 nanotubes mm^{-2}. The large contact area induces a strong interacting force between the water droplet and the PS nanotube films. The mechanism described here is similar to the one geckos use in Nature.[105,106] The difference is that the latter interactions are between two solids.

A similar phenomenon was also observed on the surface of a methyloctyldimethoxysilane (MODMS) self-assembled sili-

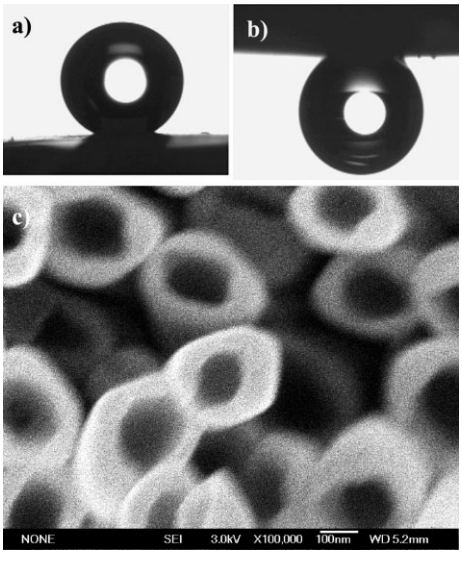

Figure 8. Superhydrophobic aligned PS nanotube films with high adhesive force. Shapes of the water droplets on the as-prepared PS nanotube films at tilt angles of a) 0° and b) 180°. c) SEM top image of the as-prepared aligned PS nanotubes films. Reprinted from [104].

con wafer.[107] The apparent CA of the MODMS-modified surface was 160.2°, while the water droplet remained unmoved on the surface even when the film was turned upside down. It is expected that these superhydrophobic films with high adhesive force to liquid could be used in the future as a "mechanical hand" to transfer small liquid droplets typical for microsample analyses.

3.3.3. Superhydrophobic Surfaces with High Electrical Conductivity

Electrical conductivity is a very important property desired for many kinds of microelectrical devices, such as light-emitting diodes, field-effect transistors, and thin-film transistors. Hydrophobic conducting materials may be very useful for corrosion protection, antistatics, and conductive textiles.[108] The original way to combine electrical properties with hydrophobicity is to electrochemically polymerize pyrrole in the presence of low-surface-energy, fluorinated molecules. The water CAs of the native polypyrrole (PPy) pellet and fluorinated PPy fabric were 96° and 110°, respectively.[109] In order to enhance the surface roughness and hydrophobicity, conductive polythiophene films with aligned microtubule structures were prepared.[110] The CA was measured to be 134°, which is much higher than those of commonly used hydrophobic materials.

Recently, conductive superhydrophobic inorganic ZnO films were prepared via the ECD method.[111] The nanopores of the surface (Fig. 9), which can be attributed to the evolution of hydrogen bubbles during the negative overpotential deposition of zinc, were used to enhance the surface hydrophobicity. The conductivity of the as-deposited films was investigated using conductive atomic force microscopy (AFM), and a current-dependent scanning image of the as-prepared film at a bias voltage of 0.5 V is shown in Figure 9b. The bright area in the image implies that the film is highly conductive.

Metals such as Au, Cu, and Ag possess electrical conductivity. Combining ECD with LbL methods, Zhang and co-workers prepared metal Ag and Au clusters.[16,72,112] The films show

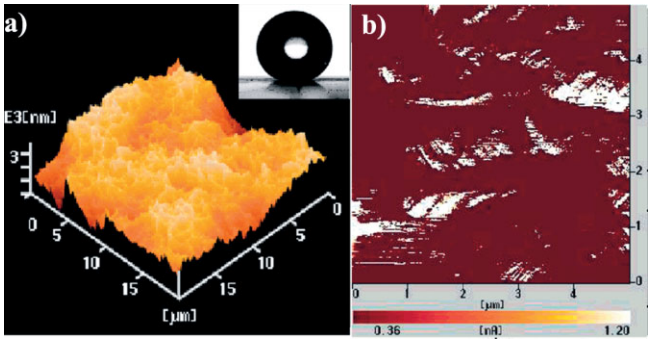

Figure 9. Superhydrophobic ZnO nanoporous films with good conductivity. a) Atomic force microscopy 3D image of the as-prepared thin films. b) Simultaneous current scanning image of the as-prepared film at a bias voltage of 0.5 V. Reprinted with permission from [111]. Copyright 2003 American Chemical Society.

superhydrophobicity after further chemisorption of a low-surface-energy molecular monolayer. Additionally, a hierarchically scaled, Cu-based, superhydrophobic surface was also produced.[113] These metal-based films exhibit conductivity and superhydrophobic properties; however, the importance of such intrinsic multifunctional properties and their potential applications were neglected.

3.3.4. Anisotropic Superhydrophobic Surfaces

Anisotropic wetting is a very important property of a patterned surface.[114–116] When a liquid droplet slides off the substrate, the three-phase contact line also moves, which is associated with an energy barrier. The length and continuity of the three-phase contact line have a great influence on the sliding behavior of the liquid droplet.[117] For a surface with 1D groove structures, the three-phase line toward the parallel direction is continuous and short, while it is longer and discontinuous in the orthogonal direction. Thus, the SA in the parallel direction is lower than in the orthogonal direction. This phenomenon is also observed in nature. Although lotus and rice leaves both possess superhydrophobicity, the water droplet can roll freely in all directions on the surface of a lotus leaf, while it rolls more easily along the direction parallel to the rice leaf edge than along the perpendicular one.[9] SEM images indicate that the arrangements of the surface papillae are different on these two structures. On a rice leaf, the papillae are arranged anisotropically, in the direction parallel to the edges, while on a lotus leaf, the distribution of the papillae is homogeneous. Recognizing this, aligned carbon nanotube (ACNT) films with a surface structure like a rice leaf were successfully prepared by controlling the surface deposition of the catalyst, and a similar anisotropic wetting phenomenon was observed.[11] It can be found that the anisotropic surface structure has great influence on the wettability. Therefore, for the preparation of surfaces with a low SA, designing a surface with a continuous, short, three-phase contact line (a low energy gap) is more effective than merely increasing the surface roughness.

The above results show the influence of the 1D surface structure on the wettability. In fact, the 2D and 3D anisotropic structure also greatly affect the surface wetting behavior. Recently, films with 3D anisotropic structuring composed of horizontal and vertical ACNT arrays were prepared.[118] These different arrangements of the components have a strong effect on the spreading behavior of the water droplets. The wettability could be switched from hydrophilic to superhydrophobic by simply adjusting the structural parameter. The anisotropic antiwetting and wetting behaviors that are induced by 1D, 2D, or 3D anisotropic structures may bring interesting insights to the design of novel microfluidic devices in the future.

3.3.5. Superhydrophobic Surfaces over the Entire pH Range

Commonly, the water used for the evaluation of surface superhydrophobicity is about pH 7,[119] and few films have

ADVANCED MATERIALS

been reported to be superhydrophobic when exposed to different pH environments. Graphitelike carbon has intrinsic thermal and chemical resistances, so it can be used in strongly acidic or basic environments.[120] Recently, we prepared nanostructured carbon films by pyrolyzing nanostructured polyacrylonitrile (PANI) films.[121] As shown in Figure 10, the films show superhydrophobicity in nearly the entire pH range. Such an unique property can be ascribed to the formation of graphitelike surface nanostructures. In addition, after the as-prepared films were dipped into strong alkaline or acid solutions for 24 h, no changes in either structure or hydrophobicity were found. This example of a superhydrophobic surface over the entire pH range gives us great inspiration for the preparation of more practically applicable interface materials.

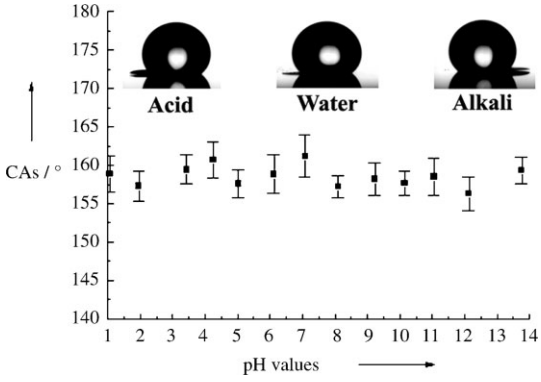

Figure 10. The relationship between pH values and contact angles on nanostructured graphitelike carbon films. The high contact angle of the acid, water, and alkali on the film indicates that the as-prepared film is superhydrophobic over the entire pH range. Reprinted from [121].

4. Superamphiphobic Surfaces

In addition to water, there are many kinds of liquids, such as oil, that are frequently used in daily life. Therefore, surfaces with both water- and oil-repellent properties would be welcome. According to Tsujii et al., in order to obtain a hydrophobic surface (CA > 90°), the surface tension of the solid substrate γ_S must be smaller than $\gamma_L/4$ of the liquid.[122] Typical surface tension of oils are about 30 mN m^{-1}. For example, the surface tensions of a rapeseed-oil droplet and of hexadecane are about 35 mN m^{-1} and 27.5 mN m^{-1}, respectively. Therefore, the critical surface tension γ_C of the solid substrate should be several mN m^{-1}.

The first example of a superamphiphobic surface was prepared by utilizing an anodically oxidized fractal structured aluminum plate.[20] After the solid surface was modified with a hydrophobic molecule (1*H*,1*H*,2*H*,2*H*-perfluorooctyltrichlorosilane), the substrate showed superhydrophobicity with a water CA of 160°, while after modification with fluorinated monoalkyl phosphates (1*H*,1*H*,2*H*,2*H*-perfluorodecyl and perfluorododecyl phosphate), the film shows superoleophobicity with a CA for rapeseed-oil droplets as high as 150°. Recently, we prepared ACNT films,[123] whereby the as-grown fresh ACNT films are superhydrophobic and superoleophilic with contact angles for water and rapeseed oil at ca. 160° and 0°, respectively. (A detailed discussion on these properties can be found in Section 6.) This indicates that the surface free energy of ACNTs is not low enough. In order to obtain a film with superamphiphobic properties, the ACNTs were further treated with fluoroalkylsilane, a material with extremely low surface energy. After the surface modification, the contact angles were ca. 171° and ca. 161° for water and rapeseed oil, respectively.

The above methods are time consuming, and real-world applications of these surfaces are very limited. Recently, by using two commonly available polymer materials, poly(methyl methacrylate) (PMMA) and fluorine-end-capped polyurethane, a one-step casting process for the preparation of superamphiphobic films was reported.[124] The as-prepared polymer films exhibit both superhydrophobic and superoleophobic properties without any further surface modification. Yabu et al. reported another simple method for the preparation of superamphiphobic surfaces from fluorinated polymers by water-assisted self-organization.[125] The as-prepared films show both superhydrophobicity for water and oleophobicity for benzene. This method has several advantages over others, including large-scale and wide-scope applicability, low cost, and low energy consumption.

5. Superamphiphilic Surfaces

Like surfaces with superamphiphobic properties, surfaces that possess superamphiphilicity (contact angles for water and oil both almost 0°) have also aroused great interest in the past several years because of their importance for practical applications. For example, superamphiphilicity could improve comfort, perspiration efficiency, and permeability in textile applications. Commonly, there are two approaches to prepare such surfaces, one based on the 2D capillary effect,[9] and the other based on the 3D capillary effect.[19]

5.1. 2D Capillary Effect

After the discovery of UV-induced superamphiphilicity on TiO_2 surfaces in 1997,[126] many research efforts have been devoted to exploring the surface photosensitive mechanism of various metal oxides.[127,128] The reason for the generation of surface superamphiphilicity has been revealed as follows: after UV illumination, oxygen vacancies in the surface are created, and these induce the conversion of the corresponding Ti^{4+} sites to Ti^{3+}. The as-formed Ti^{3+} sites are favorable for dissociated water, and further monolayers or multilayers water are formed by molecular adsorption. These reactions result in the formation of surface hydrophilic domains and leave the rest of the surface area oleophilic.[129]

Such surface-structure changes play an important role in superamphiphilicity. According to high-resolution friction

force microscopy (FFM) topographic images, the oleophilic areas are lower in position than the hydrophilic domains. Therefore, the oleophilic and hydrophilic walls might form channels for water and oil flow, respectively, which resembles a 2D capillary phenomenon. In addition, the as-induced hydrophilic and oleophilic domains are alternately arranged and have a high adhesion force for water and oil, respectively. When a liquid droplet contacts such a film, it will spread out on the film, following the "as-formed channels," to form a thin liquid film.

5.2. 3D Capillary Effect

Although the 2D capillary effect can result in superamphiphilic surfaces, the width of the as-induced flow channels are narrow (0.4–6 nm) and the mechanism is only applicable for metal oxide semiconductors with surface photosensitivity. Recently, based on the 3D capillary effect, Bico et al. proposed another, more widely applicable mechanism to prepare superamphiphilic surfaces.[19,130]

For a hydrophilic solid substrate, the liquid–solid contact is commonly governed by the Wenzel mode, and the hydrophilicity will be enhanced by the surface roughness. Typically, if the CA on the flat surface is lower than a threshold value θ_{T2}, the liquid droplet will be imbibed into the grooves of the rough surface and leaves the top of the substrate dry, which comprises fraction f_s of the total area. Combining with Young's equation, such wicking criterion can be addressed in Equation 10

$$\cos\theta_{T2} > (1-f_s)/(r-f_s) \quad (10)$$

According to this equation, if the condition $\theta < \theta_{T2}$ is fulfilled, superamphiphilic surfaces can be obtained.

Practically, in many situations, the 2D and 3D capillary effects can coexist and work cooperatively. For example, on a TiO_2 microfiber–nanoparticle composite nonwoven film, an ultrafast wetting property has been obtained. The water or oil droplet spread out rapidly within several seconds. Based on the cooperation of the 2D and 3D capillary effect, the films of lotuslike TiO_2 nanorod films and aligned ZnO nanorod films that show good superamphiphilicity have also been reported, which will be discussed in Section 7.1.

6. Surfaces with Superhydrophobicity and Superoleophilicity

Through the combination of surface superhydrophobicity with superoleophobicity, and of superhydrophilicity with superoleophilicity, surfaces with superamphiphobicity and superamphiphilicity, respectively, have been realized. In this Section, by combining superhydrophobicity with superoleophilicity, another special surface wettability that can be used to separate oil from water, or water from oil, is introduced. The surface tension of water is commonly much larger than that of oil. Therefore, if the surface tension of a solid substrate lies between those of water and oil, it might show hydrophobicity and oleophilicity. Combined with an appropriate surface design, surfaces that exhibit superhydrophobicity and superoleophilicity can be prepared.[21]

Films with these properties were prepared by coating polytetrafluoroethylene (PTFE), a hydrophobic and oleophilic material, onto a stainless steel (SS) mesh via a spray-and-dry method.[21] Detailed SEM images indicate that the as-prepared mesh films exhibit micro- and nanoscale composite rough surface structures. The water CA on the PTFE-coated mesh films is about 156°, indicating that the film is superhydrophobic. However, when a diesel oil droplet contacts it, the oil spreads on the film and permeates through the film within 240 ms, showing good superoleophilicity (Fig. 11). This kind of film has already been applied in many situations to separate water from oil or oil from water.

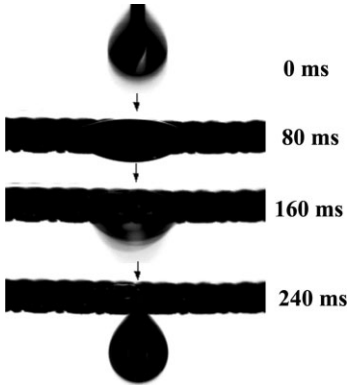

Figure 11. PTFE-coated copper mesh and its extreme wettability response for oil/water. The as-prepared films show superhydrophobicity, while, when a diesel oil droplet contacts it, the oil spreads quickly on the film and permeates through the film within 240 ms, showing good superoleophilicity. Reprinted from [21].

Compared with surfaces with superamphiphilicity or superamphiphobicity, we believe that films with the properties described in this section are more interesting and important for future applications. However, only a few experiments have been reported so far. For example, the separation of oil (water) from water (oil) based on such a film has only been studied qualitatively—that is, the real separation efficiency was not known. Therefore, a detailed quantitative study should be performed.

7. Surfaces with Reversible Superhydrophobicity and Superhydrophilicity

Stimuli-responsive materials with their surface free energy or morphology sensitive to the external environment are being used to alter the surface wettability. To date, surfaces with reversible wettability have been achieved by various

methods, including light irradiation,[131] electric-field[26] or thermal treatments,[132] and solvent treatments.[29] However, the range of the wettability transition is usually very limited; for example, the maximum water CA change of polymer-modified, photosensitive azobenzene smooth surfaces is only $11 \pm 1°$.[24]

To amplify the range of the transition, we combined the special surface morphology of copper films with the modification of attached monolayers of *n*-alkanoic acids, $CH_3(CH_2)_nCOOH$ ($n = 1, 2, 3, ..., 16$). In this way,[71] a method to tune the surface wettability between superhydrophobicity and superhydrophilicity is achieved. The wettability of rough copper films was tuned from 0° to 160° by increasing the chain length of the *n*-alkanoic acids (Fig. 12). In contrast, the wettability of smooth copper films modified with *n*-alkanoic acids could only be adjusted between 68° and 113°. This work indicates: 1) If the surface free energy of solid substrates can be tuned, their surface wettability can also be manipulated. 2) If the surface wettability of smooth substrates can be tuned between hydrophobic and hydrophilic, their wettability can be further amplified by introducing surface roughness, which is in accord with the predictions of Wenzel's (Eq. 3) and Cassie's (Eq. 5) equations. Therefore, for stimuli-responsive surfaces, the responsive wettability can be amplified by surface structural design, which provides an opportunity to realize reversible switching between superhydrophobicity and superhydrophilicity.

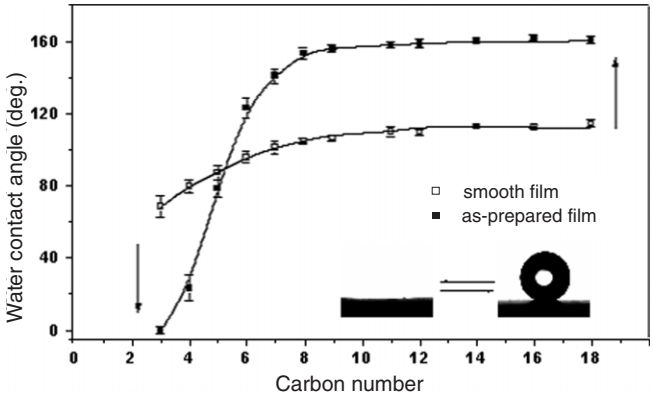

Figure 12. Relationship between the water CA and the chain length of *n*-alkanoic acids on dual-scale rough copper films that are prepared via electrodeposition. The insets show the shapes of the water droplets on films modified with *n*-propanoic acid (left) and *n*-octanoic acid (right). Reprinted from [71].

7.1. Light Irradiation

Among the methods used to control the surface wettability, light switching has received special attention because it can be controlled quickly and the switch is individually addressable. To control the wettability through light irradiation, organic compounds that show a reversible structural change triggered by light are commonly employed.[131,133–135] Spiropyrans[133] are a class of organic photochromic materials that undergo a reversible transition between the closed nonpolar form and the highly polar open form when irradiated alternately with UV (365 ± 10 nm) and visible light (450–550 nm). The water CA change of a rough Si nanowire surface coated with spiropyran molecules is 23°, which is much larger than the 12° change of the smooth surface.[134] In addition to the spiropyran molecular change, the photoswitched trans- and cis-isomers of azobenzenes can also correspond to different dipole moments and surface wettabilities. Using a simple electrostatic self-assembly technique, we modified aligned Si column substrates with a photosensitive azobenzene monolayer.[135] After UV and visible-light irradiation, the as-prepared rough films showed a CA change of 66°, compared with only about 2° on flat films. These results confirm that increasing the surface roughness can be an effective tool to amplify the CA switching range.

Compared to organic materials, inorganic materials exhibit better light, thermal, and chemical stabilities. Among photosensitive inorganic materials, titanium dioxide and zinc oxide are the most studied semiconductors.[128] On a flat ZnO substrate, the CA can change from 109° to 10° by UV illumination, the result of an UV-induced surface 2D capillary effect, as described in Section 5.1; long-term dark storage can reconvert the surface into its original hydrophobic state. However, for aligned ZnO nanorod rough films[30] (Fig. 13a), the hydrophobicity increases to superhydrophobicity under dark storage, while the hydrophilicity changes to superhydrophilicity via UV irradiation because of the cooperation of the surface 2D and 3D capillary effects (Fig. 13c). A similar remarkable surface-wettability transition was also observed on rough ZnO nanostructured films prepared via CVD[31,136] solution-

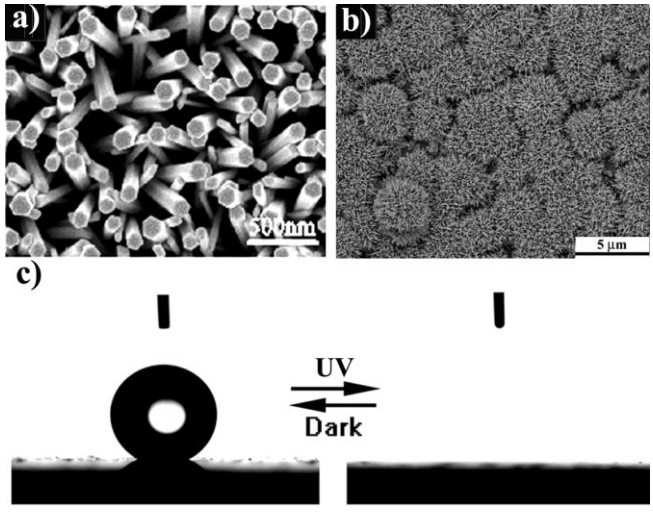

Figure 13. Reversible switching between superhydrophobicity and superhydrophilicity of inorganic nanorod films. a) Field-emission SEM top image of the as-prepared ZnO nanorod film. b) Lotuslike TiO_2 nanorod film. Reprinted with permission from [138]. Copyright 2005 Royal Society of Chemistry. c) Changes in the water-droplet shape on aligned ZnO nanorod films before (left) and after (right) UV illumination. Reprinted with permission from [30]. Copyright 2004 American Chemical Society.

dipping template methods[137] and a mild solution approach,[138] as well as on lotuslike TiO_2 nanostructured films prepared via hydrothermal (Fig. 13b)[139] and photoelectrochemical etching methods.[140] The reversible generation and annihilation of photogenerated surface oxygen defect sites cause the change of the surface free energy and the alteration of surface wettability. Their special surface micro-/nanoscale composite structures further amplify these properties.

7.2. Thermal Response

Reversible control of the surface wettability via thermal treatment has also aroused great interest in recent years.[141,142] Poly(*N*-isopropylacrylamide) (PNIPAAm) is a typical example of a thermally responsive polymer that has a lower critical solution temperature (LCST) of about 32–33 °C.[32] On a PNNIPAAm-modified flat substrate, the CA could be switched between hydrophobicity and hydrophilicity as the temperature passed through the LCST, which is the result of the competition between intra- and intermolecular hydrogen bonding (Fig. 14a). When the polymer was modified on a rough surface, the wettability could be changed from 0° to 149.3° as the temperature was elevated from 25 °C to 40 °C (Fig. 14b), which indicates that reversible switching between superhydrophobicity and superhydrophilicity has been realized by thermal treatment.

By modifying a PNIPAAm polymer on a nanostructured anodic alumina substrate, Fu et al. revealed a more detailed wettability transition mechanism.[143] As visualized by AFM, the quantitative correlation of the surface structure changes to the macroscopic water CA changes was obtained. On the basis of their observations, the wettability switch is likely caused not only by the change in surface hydrophobicity and hydrophilicity but also by the change in the surface nanoscopic topography as the temperature passes through the LCST.

In addition to soft polymer films, a range of hard materials also show a thermal response. Hard foamy films were prepared by condensing organo-triethoxysilane in a mixture of an organic solvent and water.[144] On the as-prepared substrate, a different wetting behavior to that of the PNIPAAm-modified films was observed. As is known, when the temperature is elevated, the wettability of a PNIPAAm-modified rough substrate changes from superhydrophilicity to superhydrophobicity,[32] while for the hard foamy materials the wettability changes from superhydrophobicity to superhydrophilicity. The reason for this wetting transition is the reversible crosslinking of the silica backbone, which induces a redistribution of the organic groups from the surface to the bulk of the material.

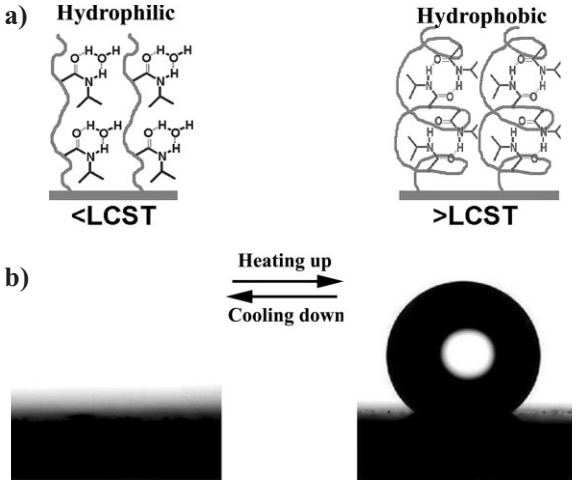

Figure 14. a) Schematic diagram of the reversible competition between inter- and intramolecular hydrogen bonding, which is the molecular mechanism of the temperature-responsive switching on a PNIPAAm film. b) Water-drop profile for thermally responsive switching between superhydrophobicity and superhydrophilicity of PNIPAAm-modified micro- and nanostructured Si surfaces at 25 °C (left) and 40 °C (right), respectively. Reprinted from [32].

7.3. Solvent Effect

When mixed polymer brushes that contain incompatible hydrophobic and hydrophilic components are attached to a substrate, the top morphology and composition of the films can be switched by exposure to different solvents, which in turn results in changes of the surface energy and the water CA.[145,146]

To verify this idea, a type of Y-shaped molecule composed of hydrophobic polystyrene and hydrophilic poly(acrylic acid) (PAA) chains was designed and grafted to a silicon surface.[147,148] After the film was treated with toluene, a good solvent for PS, the top surface layer was enriched with PS arms, whereas the PAA arms collapsed into cores. Therefore, the surface wettability could be manipulated via treatment with a selected solvent. Similarly, Minko and co-workers[33,149] attached polymer chains of PSF-COOH (PSF: pentafluorostyrene) and PVP-COOH (PVP: poly(*N*-vinylpyrrolidone)) to flat and rough PTFE substrates functionalized with hydroxyl and amino groups. Upon exposure to toluene, the top of the film was predominantly composed of the PSF component, while upon exposure to water (pH 3) the PSF formed round domains and was buried in the PVP matrix. As a result, the advanced water contact angle was reversibly tuned between 118° and 25° on a flat substrate and between 160° and about 0° on a two-level-structured rough substrate.

Among the solvent-responsive surfaces, materials with their wettability sensitive to water of different pH values are also very important. Zhang and co-workers prepared micro- and nanoscale rough gold surfaces via an electrodeposition method,[34] after which they attached a mixed monolayer containing $HS(CH_2)_9CH_3$ and $HS(CH_2)_{10}COOH$ to it. When the surface was exposed to an acidic liquid (pH 1), it showed superhydrophobicity, while when a basic liquid (pH 13) was

applied, the film showed superhydrophilicity. Very recently, a rough gold substrate was modified with 1-(11-mercaptoundecanamido)benzoic acid by the same group, and a similar pH response was observed.[150] The reason behind such pH-responsive wetting behavior is the reversible protonation and deprotonation of the surface carboxylic acid groups.

7.4. Electric-Field Response

The change of surface chemical composition provides a valuable way to control the surface wettability. However, the practical applications are limited because in many cases it is desirable to keep the composition of both the solid surface and the liquid unchanged. To achieve this, electrical-potential stimulation is a convenient method. Similar to the light-induced cis–trans reversible conformational transition of azobenzene molecules, ionizable alkanethiolates can undergo a reversible conformational reorientation by changing the applied electrical potential, which offers a new way to control the surface wettability.[151] Using this method, the density of the as-assembled alkanethiols must be controlled because a sufficient space for the molecular conformational transition is required.

Via an electrical-potential stimulus molecules can be reversibly attached onto a substrate, another way to control the surface wettability.[152] The mechanism is based on competition between the desorption and re-formation of self-assembled monolayers in solution. The surface wettability can be tuned reversibly between hydrophobicity and hydrophilicity within a few seconds.

A third method to control the surface wettability based on an external electrical field is electrowetting.[153–156] The mechanism of this method is based on an electrostatic effect. When a voltage is applied between the liquid droplet and the underlying conducting layer of a solid substrate, charges will build up both at the liquid side and at the solid electrode, causing a decrease in interfacial energy and resulting in a change of wettability from hydrophobicity to hydrophilicity. Although some results of electro-wetting, transition-induced surface wettability have been reported to date, it is still difficult to achieve electro-wetting on superhydrophobic surfaces. Recently, Krupenkin et al. proposed a method to tune the surface wettability between superhydrophobic and superhydrophilic wettability based on electro-wetting.[157] They deposited a thin polymer layer with a low surface energy on nanostructured silicon wafer surfaces. The low degree of surface roughness can not cause enough spatial separations that impede the electro-wetting effect. Before the voltage was applied, the surface showed superhydrophobicity, but the liquid droplet spread out on the film when the applied voltage exceeded a threshold.

Herein, it is worthy to note that similar to an electrical potential, a magnetic field[158] can also be a convenient method to control the surface wettability, and a magnetic superhydrophobic polyaniline nanofiber film has already been prepared via the EHD method in our lab.[159]

7.5. Mechanical Force Induction

The surface wettability of a solid substrate is governed by both the surface free energy and the surface geometrical structure. As described above, tuning the surface free energy via light illumination, thermal treatment, solvent inducement, or an electrical-field stimulus can be used to reversibly control the surface wettability. On the other hand, if the surface geometric structure of the solid substrate can be reversibly manipulated, its surface wettability can also be reversibly tuned.

PTFE is one of many elastic materials with a water CA of 108° on a flat surface. When it was extended axially with an extension ratio change from 0 to 190 %, the water CA increased from 108° to 165° and the wettability changed from hydrophobicity to superhydrophobicity.[36] The reason for this change in wettability is due to the change of the density of the PTFE crystals during the axial extension. Recently, another novel method to generate reversible wettability was reported that works by biaxially extending and unloading an elastic polyamide film.[160] When the elastic polyamide films are biaxially extended to a extension ratio larger than 120 %, the water droplet spreads out on the films. After unloading, the surface microstructures recover to their original state and the wettability returns to its superhydrophobicity. In addition to the elastomers, the surface morphology of many shape-memory materials can also be tuned reversibly via external stimuli, which could make them very useful for controlling surface wettability in future practical applications.

The controllable switching of the surface wettability between superhydrophobicity and superhydrophilicity driven by external stimuli are of great interest because these intelligent surfaces hold great promise in designing microfluidic switches, biochips, controllable drug-release systems, sensor devices, and so on.

8. Outlook and Summary

In this Review, we have presented some recent studies on functional surfaces with special wetting behaviors, such as superhydrophobicity, superhydrophilicity, superamphiphobicity, superamphiphilicity, superhydrophobicity/superoleophilicity, and reversible superhydrophobicity and superhydrophilicity, from natural to artificial surfaces and from fundamental theories to practical applications. These surfaces hold great promise for the development of various industrial products. On the other hand, the wetting behaviors of solid surfaces are complex, and they affect various other surface properties. We think that basic research on functional surfaces with controllable wettability has just started, and further detailed investigations in this field are expected.

With millions of years of evolution, creatures in Nature possess interesting and mysterious properties that we do not yet know. Therefore, further exploration and explanation of surfaces with special wetting behavior in nature is necessary. Learning from Nature will give us inspiration to develop sim-

ple and low-cost methods to construct artificial functional surfaces. In addition to fundamental research, the applications of solid substrates with special wettability are also very important. From the fundamental theories, it can be found that fabricating a surface with superhydrophobicity or superhydrophilicity requires a rough surface structure. However, the surfaces will show worse mechanical stability with increasing roughness, which is the crucial problem for their practical applications.[161] Therefore, the question of how to improve the mechanical stability of functional rough surfaces will be an important one in the future.

Solid substrates whose surface wettability can be reversibly switched have attracted much attention in recent years because of their importance in the fabrication of smart devices. We believe that more attention will be paid to this field in the near future. The design, synthesis, and application of new kinds of organic or inorganic materials with stimuli-responsive properties will be an essential and important task to fulfill. In addition, the surfaces described in this review are responsive to only one kind of external stimulus at a time, such as light, temperature, or solvent. To work in the complex conditions of a real environment, intelligent materials with a surface wettability that can be tuned by dual or multiple external stimuli, such as a combination of temperature and solvent, light and temperature, solvent and light, temperature, electric, and magnetic fields, and so on, will be necessary.

Received: September 15, 2005
Revised: February 13, 2006
Published online: November 10, 2006

[1] R. N. Wenzel, *Ind. Eng. Chem.* **1936**, *28*, 988.
[2] A. B. D. Cassie, S. Baxter, *Trans. Faraday Soc.* **1944**, *40*, 546.
[3] R. Blossey, *Nat. Mater.* **2003**, *2*, 301.
[4] A. Nakajima, K. Hashimoto, T. Watanabe, *Monatsh. Chem.* **2001**, *132*, 31.
[5] Y. Liu, L. Mu, B. H. Liu, J. L. Kong, *Chem. Eur. J.* **2005**, *11*, 2622.
[6] I. P. Parkin, R. G. Palgrave, *J. Mater. Chem.* **2005**, *15*, 1689.
[7] T. L. Sun, L. Feng, X. F. Gao, L. Jiang, *Acc. Chem. Res.* **2005**, *38*, 644.
[8] D. Öner, T. J. McCarthy, *Langmuir* **2000**, *16*, 7777.
[9] R. Wang, K. Hashimoto, A. Fujishima, M. Chikuni, E. Kojima, A. Kitamura, M. Shimohigoshi, T. Watanabe, *Adv. Mater.* **1998**, *10*, 135.
[10] W. Barthlott, C. Neinhuis, *Planta* **1997**, *202*, 1.
[11] L. Feng, S. H. Li, Y. S. Li, H. J. Li, L. J. Zhang, J. Zhai, Y. L. Song, B. Q. Liu, L. Jiang, D. B. Zhu, *Adv. Mater.* **2002**, *14*, 1857.
[12] X. F. Gao, L. Jiang, *Nature* **2004**, *432*, 36.
[13] S. Shibuichi, T. Onda, N. Satoh, K. Tsujii, *Langmuir* **1996**, *12*, 2125.
[14] J. T. Han, X. R. Xu, K. W. Cho, *Langmuir* **2005**, *21*, 6662.
[15] N. J. Shirtcliffe, G. McHale, M. I. Newton, C. C. Perry, *Langmuir* **2003**, *19*, 5626.
[16] X. Zhang, F. Shi, X. Yu, H. Liu, Y. Fu, Z. Q. Wang, L. Jiang, X. Y. Li, *J. Am. Chem. Soc.* **2004**, *126*, 3064.
[17] N. J. Shirtcliffe, G. McHale, M. I. Newton, G. Chabrol, C. C. Perry, *Adv. Mater.* **2004**, *16*, 1929.
[18] K. K. S. Lau, J. Bico, K. B. K. Teo, M. Chhowalla, G. A. J. Amaratung, W. I. Milne, G. H. McKinley, K. K. Gleason, *Nano Lett.* **2003**, *3*, 1701.
[19] J. Bico, C. Tordeux, D. Quéré, *Europhys. Lett.* **2001**, *55*, 214.
[20] S. Shibuichi, T. Yamamoto, T. Onda, K. Tsujii, *J. Colloid Interface Sci.* **1998**, *208*, 287.
[21] L. Feng, Z. Y. Zhang, Z. L. Mai, Y. M. Ma, B. Q. Liu, L. Jiang, D. B. Zhu, *Angew. Chem. Int. Ed.* **2004**, *43*, 2012.
[22] T. P. Russel, *Science* **2002**, *297*, 964.
[23] D. B. Crevoisier, P. Fabre, J. M. Corpart, L. Leibler, *Science* **1999**, *285*, 1246.
[24] K. Ichimura, S. K. Oh, M. Nakagawa, *Science* **2000**, *288*, 1624.
[25] C. L. Feng, Y. J. Zhang, J. Jin, Y. L. Song, L. Y. Xie, G. R. Qu, L. Jiang, D. B. Zhu, *Langmuir* **2001**, *17*, 4593.
[26] J. Lahann, S. Mitragotri, T. Nran, H. Kaido, J. Sundaram, I. S. Choi, S. Hoffer, G. A. Somorjai, R. Langer, *Science* **2003**, *299*, 371.
[27] B. A. Buchholz, E. A. S. Doherty, M. N. Albarghouthi, F. M. Bogdan, J. M. Zahn, A. E. Barron, *Anal. Chem.* **2001**, *73*, 157.
[28] N. Nath, A. Chilkoti, *Adv. Mater.* **2002**, *14*, 1243.
[29] S. H. Anastasiadis, H. Retsos, S. Pispas, N. Hadjichristidis, S. Neophytides, *Macromolecules* **2003**, *36*, 1994.
[30] X. J. Feng, L. Feng, M. H. Jin, J. Zhai, L. Jiang, D. B. Zhu, *J. Am. Chem. Soc.* **2004**, *126*, 62.
[31] H. Liu, L. Feng, J. Zhai, L. Jiang, D. B. Zhu, *Langmuir* **2004**, *20*, 5659.
[32] T. L. Sun, G. J. Wang, L. Feng, B. Q. Liu, Y. M. Ma, L. Jiang, D. B. Zhu, *Angew. Chem. Int. Ed.* **2004**, *43*, 357.
[33] S. Minko, M. Müller, M. Motornov, M. Nitschke, K. Grundke, M. Stamm, *J. Am. Chem. Soc.* **2003**, *125*, 3896.
[34] X. Yu, Z. Wang, Y. Jiang, F. Shi, X. Zhang, *Adv. Mater.* **2005**, *17*, 1289.
[35] L. B. Xu, W. Chen, A. Mulchandani, Y. Yan, *Angew. Chem. Int. Ed.* **2005**, *44*, 6009.
[36] J. L. Zhang, J. Li, Y. C. Han, *Macromol. Rapid Commun.* **2004**, *25*, 1105.
[37] A. W. Adamson, A. P. Gast, *Physical Chemistry of Surfaces*, Wiley, New York **1997**.
[38] J. Bico, C. Marzolin, D. Quéré, *Europhys. Lett.* **1999**, *47*, 220.
[39] A. Lafuma, D. Quéré, *Nat. Mater.* **2003**, *2*, 457.
[40] C. Ishino, K. Okumura, D. Quéré, *Europhys. Lett.* **2004**, *68*, 419.
[41] A. Marmur, *Langmuir* **2004**, *20*, 3517.
[42] A. Dupuis, J. M. Yeomans, *Langmuir* **2005**, *21*, 2624.
[43] N. A. Patankar, *Langmuir* **2003**, *19*, 1249.
[44] N. A. Patankar, *Langmuir* **2004**, *20*, 7097.
[45] J. Bico, C. Tordeux, D. Quéré, *Colloids Surf. A* **2002**, *206*, 41.
[46] M. Miwa, A. Nakajima, A. Fujishima, K. Hashimoto, T. Watanabe, *Langmuir* **2000**, *16*, 5754.
[47] G. McHale, N. J. Shirtcliffe, M. I. Newton, *Langmuir* **2004**, *20*, 10 146.
[48] C. G. L. Furmidge, *J. Colloid Sci.* **1962**, *17*, 309.
[49] R. E. Johnson, R. H. Dettre, *Adv. Chem. Ser.* **1963**, *43*, 112.
[50] C. W. Extrand, *Langmuir* **2002**, *18*, 7991.
[51] Z. Yoshimitsu, A. Nakajima, T. Watanabe, K. Hashimoto, *Langmuir* **2002**, *18*, 5818.
[52] E. Wolfram, R. Faust, *Wetting, Spreading, and Adhesion* (Ed: J. F. Padday), Academic, London **1978**, p. 213.
[53] A. R. Parker, C. R. Lawrence, *Nature* **2001**, *414*, 33.
[54] S. Herminghaus, *Europhys. Lett.* **2000**, *52*, 165.
[55] C. Neinhuis, W. Barthlott, *Ann. Bot.* **1997**, *79*, 667.
[56] P. Ball, *Nature* **1999**, *400*, 507.
[57] U. Mock, R. Förster, W. Menz, J. Rühe, *J. Phys. Condens. Matter* **2005**, *17*, S639.
[58] A. Otten, S. Herminghaus, *Langmuir* **2004**, *20*, 2405.
[59] T. Wagner, C. Neinhuis, W. Barthlott, *Acta Zool.* **1996**, *77*, 213.
[60] W. Lee, M. K. Jin, W. C. Yoo, J. K. Lee, *Langmuir* **2004**, *20*, 7665.
[61] M. H. Sun, C. X. Luo, L. P. Xu, H. Ji, Q. Ouyang, D. P. Yu, Y. Chen. *Langmuir* **2005**, *21*, 8978.
[62] C. W. Guo, L. Feng, J. Zhai, G. J. Wang, Y. L. Song, L. Jiang, D. B. Zhu, *ChemPhysChem* **2004**, *5*, 750.
[63] L. Feng, S. H. Li, H. J. Li, J. Zhai, Y. L. Song, L. Jiang, D. B. Zhu, *Angew. Chem. Int. Ed.* **2002**, *41*, 1221.
[64] L. Feng, Y. L. Song, J. Zhai, B. Q. Liu, J. Xu, L. Jiang, D. B. Zhu, *Angew. Chem. Int. Ed.* **2003**, *42*, 800.

[65] M. E. Abdelsalam, P. N. Bartlett, T. Kelf, J. Baumberg, *Langmuir* **2005**, *21*, 1753.
[66] G. Zhang, D. Y. Wang, Z. Z. Gu, H. Möhwald, *Langmuir* **2005**, *21*, 9143.
[67] J. Y. Shiu, C. W. Kuo, P. Chen, C. Y. Mou, *Chem. Mater.* **2004**, *16*, 561.
[68] J. L. Zhang, L. J. Xue, Y. C. Han, *Langmuir* **2005**, *21*, 5.
[69] Q. D. Xie, G. Q. Fan, N. Zhao, X. L. Guo, J. Xu, J. Y. Dong, L. Y. Zhang, Y. J. Zhang, C. C. Han, *Adv. Mater.* **2004**, *16*, 1830
[70] J. T. Han, D. H. Lee, C. Y. Ryu, K. Cho, *J. Am. Chem. Soc.* **2004**, *126*, 4796.
[71] S. T. Wang, L. Feng, H. Liu, T. L. Sun, X. Zhang, L. Jiang, D. B. Zhu, *ChemPhysChem* **2005**, *6*, 1475.
[72] F. Shi, Z. Q. Wang, X. Zhang, *Adv. Mater.* **2005**, *17*, 1005.
[73] H. Yan, K. Kurogi, H. Mayama, K. Tsujii, *Angew. Chem. Int. Ed.* **2005**, *44*, 3453.
[74] X. T. Zhang, O. Sato, A. Fujishima, *Langmuir* **2004**, *20*, 6065.
[75] L. Jiang, Y. Zhao, J. Zhai, *Angew. Chem. Int. Ed.* **2004**, *43*, 4338.
[76] Z. M. Huang, Y. Z. Zhang, M. Kotaki, S. Ramakrishna, *Compos. Sci. Technol.* **2003**, *63*, 2223.
[77] J. M. Deitzel, J. Kleinmeyer, D. Harris, N. C. B. Tan, *Polymer* **2001**, *42*, 261.
[78] S. Shibuichi, T. Onda, N. Satoh, K. Tsujii, *J. Phys. Chem.* **1996**, *100*, 19 512.
[79] H. Y. Erbil, A. L. Demirel, Y. Avci, O. Mert, *Science* **2003**, *299*, 1377.
[80] X. Y. Lu, C. C. Zhang, Y. C. Han, *Macromol. Rapid Commun.* **2004**, *25*, 1606.
[81] S. H. Li, H. J. Li, X. B. Wang, Y. L. Song, Y. Q. Liu, L. Jiang, D. B. Zhu, *J. Phys. Chem. B* **2002**, *106*, 9274.
[82] W. Chen, A. Y. Fadeev, M. C. Hsieh, D. Öner, J. Youngblood, T. J. McCarthy, *Langmuir* **1999**, *15*, 3395.
[83] I. Woodward, W. C. E. Schofield, V. Roucoules, J. P. S. Badyal, *Langmuir* **2003**, *19*, 3432.
[84] B. He, N. A. Patankar, J. Lee, *Langmuir* **2003**, *19*, 4999.
[85] R. M. Jisr, H. H. Rmaile, J. B. Schlenoff, *Angew. Chem. Int. Ed.* **2005**, *44*, 782.
[86] J. Genzer, K. Efimenko, *Science* **2000**, *290*, 2130.
[87] L. Zhai, F. C. Cebeci, R. E. Cohen, M. F. Rubner, *Nano Lett.* **2004**, *4*, 1349.
[88] S. Tsoi, E. Fok, J. C. Sit, J. G. C. Veinot, *Langmuir* **2004**, *20*, 10 771.
[89] X. D. Wu, L. J. Zheng, D. Wu, *Langmuir* **2005**, *21*, 2665.
[90] B. T. Qian, Z. Q. Shen, *Langmuir* **2005**, *21*, 9007.
[91] E. Hosono, S. Fujihara, I. Honma, H. Zhou, *J. Am. Chem. Soc.* **2005**, *127*, 13 458.
[92] A. Nakajima, *J. Am. Ceram. Soc.* **2004**, *87*, 533.
[93] K. Tadanaga, N. Katata, T. Minami, *J. Am. Ceram. Soc.* **1997**, *80*, 1040.
[94] A. Nakajima, A. Fujishima, K. Hashimoto, T. Watanabe, *Adv. Mater.* **1999**, *11*, 1365.
[95] A. Hozumi, O. Takai, *Thin Solid Films* **1998**, *334*, 54.
[96] Y. Y. Wu, H. Sugimura, Y. Inoue, O. Takai, *Chem. Vap. Deposition* **2002**, *8*, 47.
[97] X. J. Feng, J. Zhai, L. Jiang, unpublished.
[98] Y. Xu, W. H. Fan, Z. H. Li, D. Wu, Y. H. Sun, *Appl. Opt.* **2003**, *42*, 108.
[99] Y. Xu, D. Wu, Y. H. Sun, Z. X. Huang, X. D. Jiang, X. F. Wei, Z. H. Wei, B. Z. Dong, Z. H. Wu, *Appl. Opt.* **2005**, *44*, 527.
[100] X. T. Zhang, O. Sato, M. Taguchi, Y. Einaga, T. Murakami, A. Fujishima, *Chem. Mater.* **2005**, *17*, 696.
[101] M. S. Park, Y. Lee, J. K. Kim, *Chem. Mater.* **2005**, *17*, 3944.
[102] A. Nakajima, K. Hashimoto, T. Watanabe, K. Takai, G. Yamauchi, A. Fujishima, *Langmuir* **2000**, *16*, 7044.
[103] Z. Z. Gu, H. Uetsuka, K. Takahashi, R. Nakajima, H. Onishi, A. Fujishima, O. Sato, *Angew. Chem. Int. Ed.* **2003**, *42*, 894.
[104] M. H. Jin, X. J. Feng, L. Feng, T. L. Sun, J. Zhai, T. J. Li, L. Jiang, *Adv. Mater.* **2005**, *17*, 1977.
[105] K. Autumn, Y. A. Liang, S. T. Hsieh, W. Zesch, W. P. Chan, T. W. Kenny, R. Fearing, R. J. Full, *Nature* **2000**, *405*, 681.
[106] A. K. Geim, S. V. Dubonos, I. V. Grigorieva, K. S. Novoselov, A. A. Zhukov, S. Y. Shapoval, *Nat. Mater.* **2003**, *2*, 461.
[107] X. Y. Song, J. Zhai, Y. L. Wang, L. Jiang, *J. Phys. Chem. B* **2005**, *109*, 4048.
[108] G. Kousik, S. Pitchumani, N. G. Renganathan, *Prog. Org. Coat.* **2001**, *43*, 286.
[109] D. Mecerreyes, V. Alvaro, I. Cantero, M. Bengoetxea, P. A. Calvo, H. Grande, J. Rodriguez, J. A. Pomposo, *Adv. Mater.* **2002**, *14*, 749.
[110] Z. Zhang, L. Gu, G. Shi, *J. Mater. Chem.* **2003**, *13*, 2858.
[111] M. Li, J. Zhai, H. Liu, Y. L. Song, L. Jiang, D. B. Zhu, *J. Phys. Chem. B* **2003**, *107*, 9954.
[112] N. Zhao, F. Shi, Z. Q. Wang, X. Zhang, *Langmuir* **2005**, *21*, 4713.
[113] N. J. Shirtcliffe, G. McHale, M. I. Newton, C. C. Perry, *Langmuir* **2005**, *21*, 937.
[114] M. Gleiche, L. F. Chi, H. Fuchs, *Nature* **2000**, *403*, 173.
[115] J. P. Youngblood, T. J. McCarthy, *Macromolecules* **1999**, *32*, 6800.
[116] H. Murase, K. Nanishi, H. Kogure, T. Fujibayashi, K. Taura, N. Haruta, *J. Appl. Polym. Sci.* **1994**, *54*, 051.
[117] Z. Yoshimitsu, A. Nakajima, T. Watanabe, K. Hashimoto, *Langmuir* **2002**, *18*, 5818.
[118] T. L. Sun, G. J. Wang, H. Liu, L. Feng, L. Jiang, D. B. Zhu, *J. Am. Chem. Soc.* **2004**, *125*, 14 996.
[119] J. D. Miller, S. Veeramasuneni, J. Drelich, M. R. Yalamanchili, G. Yamauchi, *Polym. Eng. Sci.* **1996**, *36*, 1849.
[120] K. Esumi, M. Ishigami, A. Nakajima, K. Sawada, H. Honda, *Carbon* **1996**, *34*, 279.
[121] L. Feng, Z. L. Yang, J. Zhai, Y. L. Song, B. Q. Liu, Y. M. Ma, Z. H. Yang, L. Jiang, D. B. Zhu, *Angew. Chem. Int. Ed.* **2003**, *42*, 4217.
[122] K. Tsujii, K. T. Yamamoto, T. Onda, S. Shibuichi, *Angew. Chem. Int. Ed. Engl.* **1997**, *36*, 1011.
[123] H. J. Li, X. B. Wang, Y. L. Song, Y. Q. Liu, Q. S. Li, L. Jiang, D. B. Zhu, *Angew. Chem. Int. Ed.* **2001**, *40*, 1743.
[124] Q. D. Xie, J. Xu, L. Feng, L. Jiang, W. H. Tang, X. D. Luo, C. C. Han, *Adv. Mater.* **2004**, *16*, 302.
[125] H. Yabu, M. Takebayashi, M. Tanaka, M. Shimomura, *Langmuir* **2005**, *21*, 3235.
[126] R. Wang, K. Hashimoto, A. Fujishima, M. Chikuni, E. Kojima, A. Kitamura, M. Shimohigoshi, T. Watanabe, *Nature* **1997**, *388*, 431.
[127] M. Miyauchi, A. Nakajima, T. Watanabe, K. Hashimoto, *Chem. Mater.* **2002**, *14*, 2812.
[128] R. D. Sun, A. Nakajima, A. Fujishima, T. Watanabe, A. Hashimoto, *J. Phys. Chem. B* **2001**, *105*, 1984.
[129] R. Wang, N. Sakai, A. Fujishima, T. Watanabe, K. Hashimoto, *J. Phys. Chem. B* **1999**, *103*, 2188.
[130] J. Bico, C. Tordeux, D. Quéré, *Colloids Surf. A* **2002**, *206*, 41.
[131] S. Abbott, J. Ralston, G. Reynolds, R. Hayes, *Langmuir* **1999**, *15*, 8923.
[132] D. M. Jones, J. R. Smith, W. T. Huck, C. Alexander, *Adv. Mater.* **2002**, *14*, 1130.
[133] R. Rosario, D. Gust, M. Hayes, F. Jahnke, J. Springer, A. A. Garcia, *Langmuir* **2002**, *18*, 8062.
[134] R. Rosario, D. Gust, A. A. Garcia, M. Hayes, J. L. Taraci, J. W. Dailey, S. T. Picraux, *J. Phys. Chem. B* **2004**, *108*, 12 640.
[135] W. H. Jiang, G. J. Wang, Y. N. He, X. G. Wang, Y. L. An, Y. L. Song, L. Jiang, *Chem. Commun.* **2005**, *28*, 3550.
[136] L. Huang, S. P. Lau, H. Y. Yang, E. S. P. Leong, S. F. Yu, S. Prawer, *J. Phys. Chem. B* **2005**, *109*, 7746.
[137] Y. Li, W. P. Cai, G. T. Duan, B. Q. Cao, F. Q. Sun, F. Lu, *J. Colloid Interface Sci.* **2005**, *287*, 634.
[138] S. Yin, T. Sato, *J. Mater. Chem.* **2005**, *15*, 4584.
[139] X. J. Feng, J. Zhai, L. Jiang, *Angew. Chem. Int. Ed.* **2005**, *44*, 5115.
[140] H. Irie, T. S. Ping, T. Shibata, K. Hashimoto, *Electrochem. Solid-State Lett.* **2005**, *8*, D23.
[141] D. L. Huber, R. P. Manginell, M. A. Samara, B. I. Kim, B. C. Bunke, *Science* **2003**, *301*, 352.

[142] M. Motornov, S. Minko, K. J. Eichhorn, M. Nitschke, F. Simon, M. Stamm, *Langmuir* **2003**, *19*, 8077.
[143] Q. Fu, G. V. Rama Rao, S. B. Basame, D. J. Keller, K. Artyushkova, J. E. Fulghum, G. P. Lopez, *J. Am. Chem. Soc.* **2004**, *126*, 8904.
[144] N. J. Shirtcliffe, G. McHale, M. I. Newton, C. C. Perry, P. Roach, *Chem. Commun.* **2005**, 3135.
[145] B. Zhao, W. J. Brittain, *Macromolecules* **2000**, *33*, 8813.
[146] H. Tan, T. L. Sun, J. H. Li, M. Guo, X. Y. Xie, Y. P. Zhong, Q. Fu, L. Jiang, *Macromol. Rapid Commun.* **2005**, *26*, 1418.
[147] D. Julthongpiput, Y. H. Lin, J. Teng, E. R. Zubarev, V. V. Tsukruk, *Langmuir* **2003**, *19*, 7832.
[148] D. Julthongpiput, Y. H. Lin, J. Teng, E. R. Zubarev, V. V. Tsukruk, *J. Am. Chem. Soc.* **2003**, *125*, 15 912.
[149] A. Sidorenko, S. Minko, K. Schenk-Meuser, H. Duschner, M. Stamm, *Langmuir* **2000**, *16*, 8349.
[150] Y. G. Jiang, Z. Q. Wang, X. Yu, F. Shi, H. P. Xu, X. Zhang, *Langmuir* **2005**, *21*, 1986.
[151] Y. Liu, L. Mu, B. H. Liu, S. Zhang, P. Y. Yang, J. L. Kong, *Chem. Commun.* **2004**, 1194.
[152] N. L. Abbott, C. B. Gorman, G. M. Whitesides, *Langmuir* **1995**, *11*, 16.
[153] W. J. J. Welters, L. G. J. Fokkink, *Langmuir* **1998**, *14*, 1535.
[154] H. J. J. Verheijen, M. W. J. Prins, *Langmuir* **1999**, *15*, 6616.
[155] T. B. Jones, *Langmuir* **2002**, *18*, 4437.
[156] R. A. Hayes, B. J. Feenstra, *Nature* **2003**, *425*, 383.
[157] T. N. Krupenkin, J. A. Taylor, T. M. Schneider, S. Yang, *Langmuir* **2004**, *20*, 3824.
[158] E. Katz, L. Sheeney-Haj-Ichia, B. Basnar, I. Felner, I. Willner, *Langmuir* **2004**, *20*, 9714.
[159] Y. Zhu, J. C. Zhang, J. Zhai, L. Jiang, *Thin Solid Films* **2006**, *510*, 271.
[160] J. L. Zhang, X. Y. Lu, W. H. Huang, Y. C. Han, *Macromol. Rapid Commun.* **2005**, *26*, 477.
[161] A. Nakajima, K. Abe, K. Hashimoto, T. Watanabe, *Thin Solid Films* **2000**, *376*, 140.